# Inhibition Effects of Some Polymers on Electroreduction of Anions at the Mercury/Solution Interface

Tetsuya OHSAKA, Yasuo IIDA, and Tadashi YOSHIDA

*Applied Electrochemistry Laboratory, Graduate School of Science and Engineering, Waseda University, Nishi-Okubo, Shinjuku-ku, Tokyo 160*

(Received May 8, 1974)

The present work was conducted to investigate the electroreduction of anions (typically $S_2O_8^{2-}$ and $BrO_3^-$) under the influence of the adsorption of polymers (polyethyleneglycol, alkylphenoxy polyethoxy ethanols and polyvinylpyrrolidone) on the electrode surface. The limiting current of $S_2O_8^{2-}$ reduction was depressed by the polymers in the region from nearly the zero-charge potential to the more negative potential. The half-wave potential of $BrO_3^-$ reduction shifted towards more negative potential by adding the polymers. In the potential range where the cathodic current was mainly controlled by mass transfer of the anions, the time ($t_m$) needed to complete the formation of a monolayer was obtainable conveniently from the instantaneous current *vs.* time ($I$—$t$) curve as reported previously for the inhibited reduction of $Cd^{2+}$ or $Cu^{2+}$.[2,3,8] In the potential range where the current was mainly controlled by charge transfer, an exact determination of $t_m$, by which the maximum surface concentration of polymer was given, was possible only when the instantaneous current density ($i$) was plotted against $t^{1/2}$. In such a potential range, $i$ was expressed as follows.

$$i = i_0 - (i_0 - i_1)(t/t_m)^{1/2} \quad \text{for } t \leqslant t_m$$

or

$$i = i_1 \quad \text{for } t > t_m$$

Moreover,

$$\bar{I}_{ads}/\bar{I}_0 = 1 - \frac{10}{13}\frac{i_0 - i_1}{i_0}(t_d/t_m)^{1/2} \quad \text{for } t_d \leqslant t_m$$

$$\bar{I}_{ads}/\bar{I}_0 = 1 - \frac{10}{13}\frac{i_0 - i_1}{i_0} - \frac{3}{13}\frac{i_0 - i_1}{i_0}\{1 - (t_d/t_m)^{-5/3}\} \quad \text{for } t_d > t_m$$

where $i_0$ and $i_1$ are the instantaneous current densities at $\theta=0$ and 1, $\bar{I}_{ads}$ and $\bar{I}_0$ the polarographic currents with and without polymers, $t_d$ the drop time, $t_m$ the time required to attain the saturated adsorption. The relationship between the shift of half-wave potential and $(t_d/t_m)^{1/2}$ (for $t_d \leqslant t_m$) or $(t_d/t_m)^{-5/3}$ (for $t_d > t_m$), was introduced and the results were verified for the inhibition effects of polymer on the electroreduction of $BrO_3^-$ as well as for that on $VO^{2+}$ reduction.

The adsorption of polymers at the mercury/solution interface has been investigated by differential capacity measurements,[1] and it was found that the adsorption is mainly controlled by diffusion process at the initial stage. The inhibition due to an adsorbed polymer on the electroreduction of $Cd^{2+}$ or $Cu^{2+}$ scarcely took place until the attainment of a certain high coverage when the sharp increase of inhibition occured. Such inhibition effects might be characterized by the diffusion process of depolarizer.[2,3]

The present paper is mainly concerned with the inhibition effects of polymer on the electroreduction of some anions, which will be compared with those on $Cd^{2+}$ reduction. The process of electroreduction of anion is characterized by the interference owing to the influence of electric field in the double layer on the reacting entities, and the interference arises markedly in a dilute supporting electrolyte solution.[4] In consideration of polyvalent anions including $S_2O_8^{2-}$, $Fe(CN)_6^{3-}$, and $PtCl_4^{2-}$ or monovalent anions such as $BrO_3^-$, $NO_3^-$, and $IO_3^-$ under the double layer effects,[5] the electroreduction of $S_2O_8^{2-}$ [4,6] and $BrO_3^-$ [7] will be investigated typically.

## Experimental

A DME (dropping mercury electrode) was used as the test electrode. All the potentials were referred to a saturated calomel electrode (SCE). A Yanagimoto P-8 Type Polarograph with three electrodes system was used for the measurements of current-potential curves. The instantaneous current *vs.* time curves were determined from the $iR$ drop observed with a recorder or an oscilloscope in parallel with 2 kΩ resistance which was connected in series with the DME and the polarization circuit. Water-soluble polymers PVP (BASF), PEG (Sanyo Chemical Industry), and Triton X (Rohm and Haas) were used without further purification. The depolarizers were reagent-grade $CdSO_4$, $K_2S_2O_8$, $KBrO_3$, and $VOSO_4$. Observation was carried out in the atmosphere of purified nitrogen at 25 °C.

## Results and Discussion

*Inhibition Effects of Polymer on the Electroreduction of $S_2O_8^{2-}$. For the Case Where the Current Is Mainly Controlled by Mass Transfer*: Figure 1 shows the polarograms of $S_2O_8^{2-}$ reduction inhibited by the adsorption of PVP. It was confirmed by the differential capacity measurements[1] that the adsorption of PVP occurs within the potential range in Fig. 1. The polarographic currents were inhibited in the range from the vicinity of zero-charge potential to *ca.* −1.5 V. Similarly, PEG or Triton X inhibited the reduction of $S_2O_8^{2-}$. The decrease of inhibition effects in the range from *ca.* −1.2 to −1.8 V may be ascribed to sufficient polarization. It is interesting that the inhibition effects of polymers on $S_2O_8^{2-}$ reduction are similar to the "supporting electrolyte effect"[5] which results from the double layer effects on anion reduction in the absence of adsorbates.

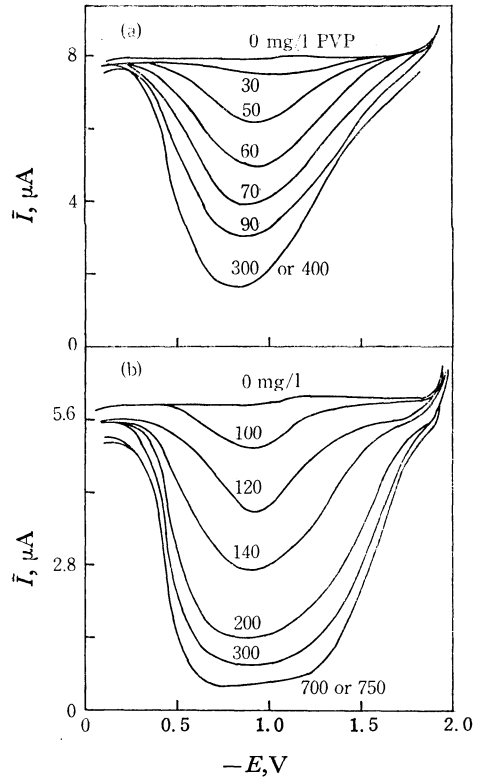


Fig. 1. Polarograms of $K_2S_2O_8$ inhibited by PVP.
(a) 0.5 M sodium sulfate+1.5 mM $K_2S_2O_8$+various contents of PVP $\bar{M}$=10000.
(b) 0.5 M sodium sulfate+1.0 mM $K_2S_2O_8$+various contents of PVP $\bar{M}$=750000.

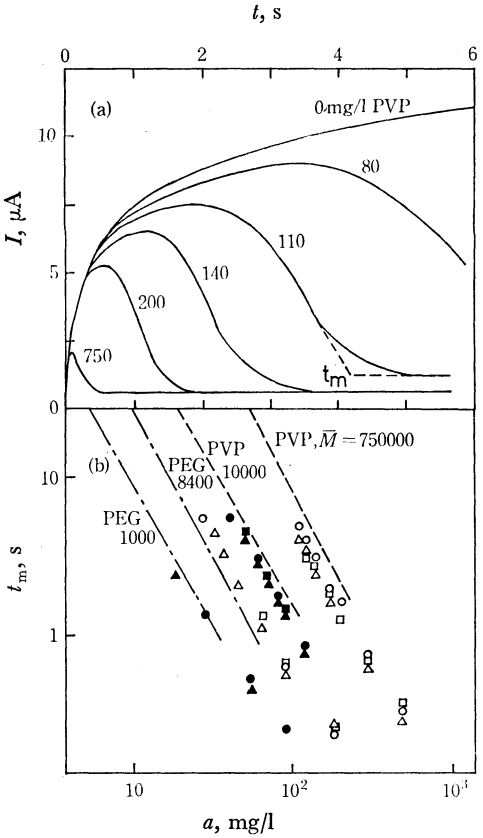


Fig. 2. Instantaneous current measurements for $K_2S_2O_8$ reduction.
(a) $I-t$ curves: 0.5 M sodium sulfate+1.0 mM $K_2S_2O_8$+various contents of PVP $\bar{M}$=750000, $E$=−0.8 V.
(b) log $t_m$ *vs.* log $a$ plots: 0.5 M sodium sulfate+1.0 mM $K_2S_2O_8$+various adsorbates, PVP $\bar{M}$=750000 observed at potentials (○: −0.4 V, △: −0.8 V, □: −1.2 V), PVP $\bar{M}$=10000 (●: −0.5 V, ▲: −1.0 V, ■: −1.5 V), PEG $\bar{M}$=8400 (○: −0.5 V, △: −0.9 V, □: −1.5 V), PEG $\bar{M}$=1000 (●: −0.5 V, ▲: −1.0 V), dashed lines for PVP observed at −0.5 V and one-dotted lines for PEG observed at −0.6 V are derived from differential capacity measurements in 0.5 M sulfuric acid.

In the case of diffusion-controlled adsorption in a dilute PVP solution, PVP of low $\bar{M}$ was more effective on the inhibition than that of high $\bar{M}$ as shown by the results for 50 mg/l of $\bar{M}$=10000 and 100 mg/l of $\bar{M}$=750000 in Fig. 1. Such results may be due to the diffusion coefficient which decreases with $\bar{M}$. On the contrary, PVP of high $\bar{M}$ took more the effect on the inhibitive action as compared with that of low $\bar{M}$ when the adsorption attained the saturation in concentrated PVP solution. The tendency similar to the cases of PVP was also revealed by PEG in the inhibition effects. However, the inhibition of Triton X became more effective with the decreases of $\bar{M}$ in each case of diffusion-controlled or saturated adsorption, which might be due to the increase of adsorbability of Triton X with the decrease of $\bar{M}$ in contrast with the cases of PVP and PEG.

We have investigated the determination of the maximum surface concentration ($\Gamma_m$) of polymer at the interface, and it was derived from the time $t_m$, at which the formation of a monolayer of polymer was achieved. The time $t_m$ required to attain the saturated adsorption of polymer was obtained previously by the differential capacity measurements,[1] while it was also determined from the time dependence of instantaneous limiting current.[2,3] Such time dependence was observed at the potential where the polarogram was most depressed. Figure 2(a) shows the instantaneous limiting current *vs.* time ($I-t$) curves for $S_2O_8^{2-}$ at $E$=−0.8 V in the solution containing PVP of $\bar{M}$=750000. These curves are similar to those in Refs. 2, 3, and 8 where the limiting current is inhibited by diffusion-controlled film formation of polymer. The time $t_m$ can be obtained conveniently by extrapolating the sharply decreasing region in $I-t$ curve to the minimum one. The plots of log $t_m$ *vs.* log $a$ ($a$: bulk concentration of adsorbates) obtained from $I-t$ curves are shown in Fig. 2(b) in comparison with those derived from the differential capacity measurements. In Fig. 2(b), the broken and one-dotted lines are derived from the capacity method,[1-3] and their slopes of *ca.* −2 are in approximate agreement with those plotted with $t_m$ values obtained from $I-t$ curves, which supports the Koryta equation[9] as described in the previous papers.[1-3] Therefore, in the case as shown in Fig. 2, $t_m$ can be conveniently determined by the instantaneous limiting current, which makes the estimation of $\Gamma_m$ (maximum surface concentration of adsorbates) easy.

*For the Case Where the Current Is Mainly Controlled by Charge Transfer*: Figure 3(a) shows the polarograms of $S_2O_8^{2-}$ in 0.005 M sodium sulfate, where the limiting

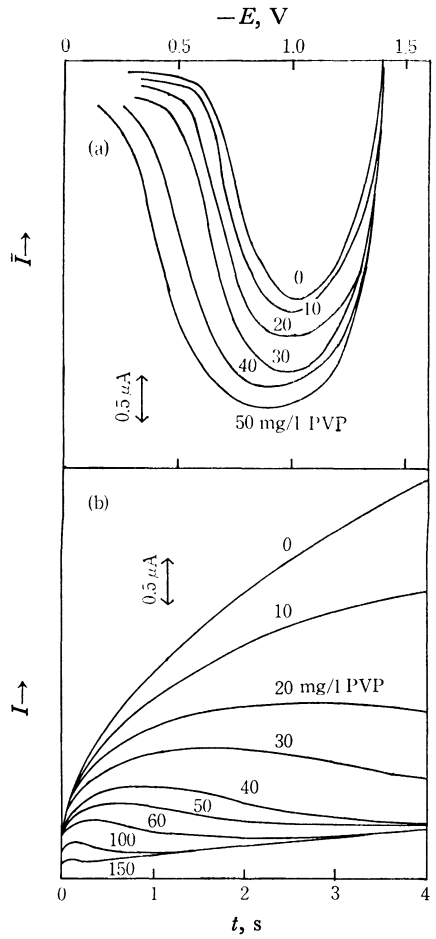


Fig. 3. Polarograms of 1.5 mM $K_2S_2O_8$ in 0.005 M sodium sulfate inhibited by PVP $\bar{M}=10000$ and their instantaneous current *vs.* time curves observed at −1.0 V.
(a) Polarograms, (b) $I-t$ curves.

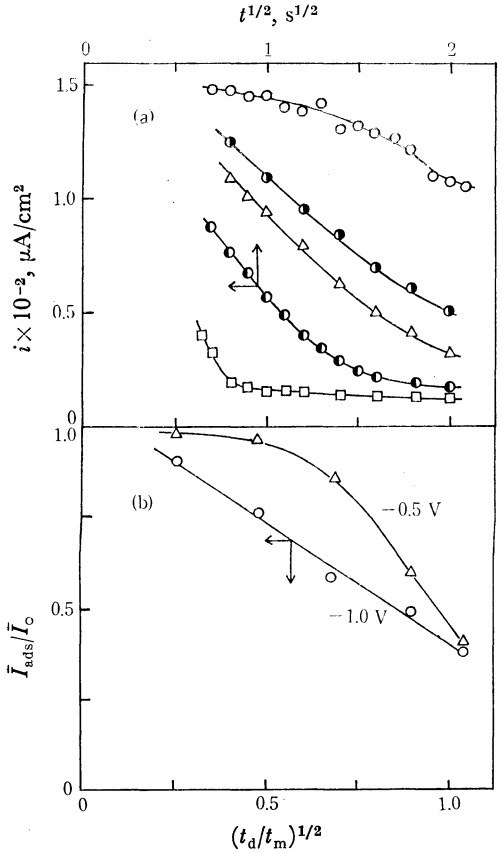


Fig. 4. Behaviors of instantaneous current density for $K_2S_2O_8$ reduction in the presence of polymer in a dilute supporting electrolyte.
1.5 mM $K_2S_2O_8$+0.005 M sodium sulfate+various contents of PVP $\bar{M}=10000$,
(a) $i-t^{1/2}$ plots at −1.0 V, contents (○: 0 mg/l PVP, ◑: 20 mg/l, △: 30 mg/l, ◐: 50 mg/l, □: 150 mg/l),
(b) $\bar{I}_{ads}/\bar{I}_0$ *vs.* $(t_d/t_m)^{1/2}$ plots at −0.5 and −1.0 V.

current without adsorbates is depressed by the double layer effects in the range from *ca.* −0.6 V to −1.4 V. In the above range, the current is mainly controlled by charge transfer rather than mass transfer.[4,5] The inhibition effects of polymer in a dilute supporting electrolyte are larger than those in a concentrated electrolyte, as shown by the results for 50 mg/l PVP in Fig. 3(a) and Fig. 1(a). The $I-t$ curves in Fig. 3(b) were observed at $E=-1.0$ V where the maximum inhibition by polymer was shown. In the $I-t$ curve without adsorbates, $I$ becomes the function of $t^{2/3}$ instead of $t^{1/6}$ which means limiting current. Further, the $I-t$ curves with adsorbates always show the ambiguous transition range from diffusion-controlled to saturated adsorption, which makes the graphical determination of $t_m$ difficult.

For the purpose of determining the time $t_m$, $I-t$ curves in Fig. 3(b) were rewritten as $i$ *vs.* $t^{1/2}$ plots in Fig. 4(a) in view of diffusion-controlled film formation. In the absence of adsorbates, the instantaneous current density somewhat decreases with time owing to the influence of diffusion process of depolarizer, though the value is expected to be constant independently of time. In the presence of adsorbates, the instantaneous current density decreases linearly with $t^{1/2}$ in the range of diffusion-controlled adsorption of polymer, whereas $i$ becomes nearly constant after the attainment of saturated adsorption. Then, the inhibition effects of polymer on the instantaneous current density in the potential range where the current is mainly controlled by charge transfer of depolarizer can be given by Eqs. (1) and (2) shown later. This tendency is similar to that of $C$ (differential capacity) *vs.* $t^{1/2}$ curves, and the time $t_m$ can be easily determined by the graphical extrapolation in the same manner as described previously for $C-t^{1/2}$ curves.[1]

*Relationship between Polarographic Current and Instantaneous Current Density.* When the current is mainly controlled by charge transfer, the inhibition is assumed to be ascribed mainly to the blocking effect of adsorbates by considering the behavior of Fig. 4(a). The instantaneous current density before the attainment of saturated adsorption can be regarded as the sum of the instantaneous current densities on the covered ($i_1$) and the "clean" areas ($i_0$) as follows.

$$i = i_0(1-\theta) + i_1\theta = i_0 - (i_0-i_1)(t/t_m)^{1/2} * \quad \text{for } t \leqslant t_m \qquad (1)$$

* $\theta = \dfrac{\Gamma}{\Gamma_m} = \dfrac{0.736D^{1/2}at^{1/2}}{0.736D^{1/2}at_m^{1/2}} = (t/t_m)^{1/2}$, where $D$ and $a$ are the diffusion coefficient and bulk concentration of adsorbates.

When the saturated adsorption is achieved,

$$i = i_1 \qquad \text{for } t > t_m \qquad (2)$$

where $i_0$ and $i_1$ are the instantaneous current densities at $\theta$ (coverage)=0 and 1. These equations are supported by three conditions for $i-t^{1/2}$ curves: (i) instantaneous current density at $t=0$ ($i_0$) becomes constant regardless of polymer concentration, (ii) instantaneous current density in the presence of adsorbates decreases linearly with $t^{1/2}$, and (iii) instantaneous current density in the case of saturated adsorption becomes constant value $i_1$.

The relation between polarographic current and instantaneous current density can be derived from Eq. (1) or (2).

For $t_d \leq t_m$

$$I = A\{i_0-(i_0-i_1)(t/t_m)^{1/2}\}$$

Then,

$$\bar{I}_{ads}/\bar{I}_0 = \frac{\frac{1}{t_d}\int_0^{t_d} 0.85(mt)^{2/3}\{i_0-(i_0-i_1)(t/t_m)^{1/2}\}dt}{\frac{1}{t_d}\int_0^{t_d} 0.85(mt)^{2/3}i_0 dt}$$

$$= 1 - \frac{10}{13}\frac{i_0-i_1}{i_0}(t_d/t_m)^{1/2} \qquad (3)$$

where $\bar{I}_{ads}$ and $\bar{I}_0$ are the polarographic currents with and without adsorbates, and $A$, $t_d$, and $m$ are the surface area ($=0.85\ m^{2/3}\ t^{2/3}$), the drop time, and the mercury flow rate, respectively.

For the purpose of investigating Eq. (3), the relation of $\bar{I}_{ads}/\bar{I}_0$ *vs.* $(t_d/t_m)^{1/2}$ was plotted in Fig. 4(b). $\bar{I}_{ads}/\bar{I}_0$ *vs.* $(t_d/t_m)^{1/2}$ curve becomes linear at $-1.0$V where the current is mainly controlled by charge transfer, whereas at $-0.5$ V it deviates from the linearity because of the mass transfer becoming predominant at $-0.5$ V.[4,5] Then, Eq. (3) holds for the system where the current being mainly controlled by charge transfer, is inhibited by polymer.

For $t_d > t_m$,

$$\bar{I}_{ads}/\bar{I}_0 = \frac{\frac{1}{t_d}\int_0^{t_m} A\{i_0-(i_0-i_1)(t/t_m)^{1/2}\}dt + \frac{1}{t_d}\int_{t_m}^{t_d} Ai_1 dt}{\frac{1}{t_d}\int_0^{t_d} Ai_0 dt}$$

$$= 1 - \frac{10}{13}\frac{i_0-i_1}{i_0} - \frac{3}{13}\frac{i_0-i_1}{i_0}\{1-(t_d/t_m)^{-5/3}\} \qquad (4)$$

Eq. (4) is expected to hold as well as Eq. (3) within the potential range where the current is mainly controlled by charge transfer.

*Inhibition Effects of Polymer on the Electroreduction of $BrO_3^-$.* Figure 5 shows the polarograms of $BrO_3^-$ reduction in 0.05 M sulfuric acid where the half-wave potential shifts from $-0.4$ V to more negative side by adding PEG, and this tendency differs from that of polarograms for $S_2O_8^{2-}$ reduction in 0.5 M sodium sulfate. The shift of half-wave potential is relatively large in a dilute polymer solution where the adsorption is controlled by the diffusion of polymer, while the shift tends to be saturated in the polymer solution so concentrated as to attain rapidly the saturated adsorption. PVP and PEG of small $\bar{M}$ have greater influence on polarograms as compared with those of large $\bar{M}$ in the range of diffusion-controlled adsorption, however, the reverse is the case in the range of saturated adsorption.

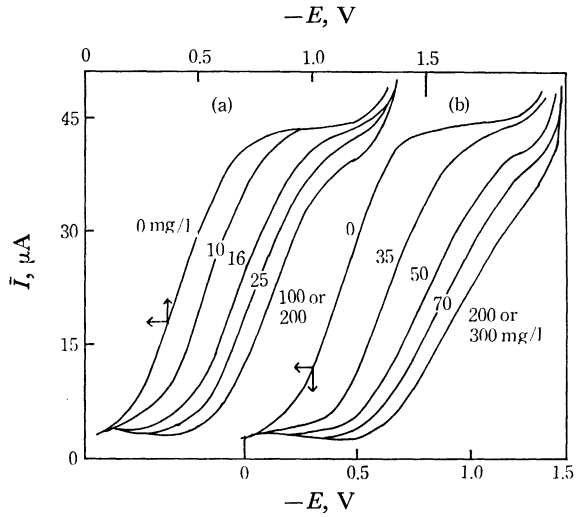


Fig. 5. Polarograms of $KBrO_3$ inhibited by PEG.
0.05 M sulfuric acid+1.0 mM $KBrO_3$+various contents of PEG,
(a) PEG $\bar{M}$=1000, (b) PEG $\bar{M}$=8400.

In the case of Triton X, the smaller the mean molecular weight ($\bar{M}$), the larger the influence on polarograms in each case of diffusion-controlled and saturated adsorption.

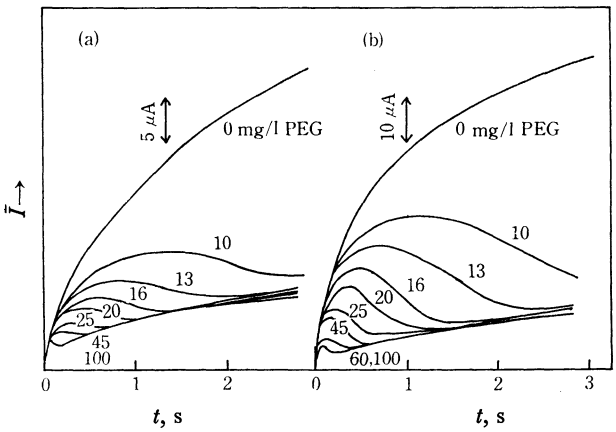


Fig. 6. Instantaneous current *vs.* time curves for $KBrO_3$ reduction inhibited by PEG.
0.05 M sulfuric acid+1.0 mM $KBrO_3$+various contents of PEG $\bar{M}$=1000,
(a) $E=-0.3$ V, (b) $E=-0.5$ V.

For the $BrO_3^-$ reduction inhibited by PEG in 0.05 M sulfuric acid, $I-t$ curves were observed at two potentials along the waves in Fig. 5; $-0.3$ V is a typical potential at the foot of polarograms (Fig. 6(a)), and $-0.5$ V is that in the neighborhood of limiting current (Fig. 6(b)). The time $t_m$ can be easily determined from $I-t$ curves at $-0.5$ V shown in Fig. 6(b) in the same way as described in Fig. 2(a). However, from the $I-t$ curves at $-0.3$ V in Fig. 6(a) the determination of $t_m$ is difficult because of the indistinct transition range from the diffusion-controlled to the saturated adsorption.

The inhibition effects of polymers on $BrO_3^-$ reduction are examined in detail at the foot of polarographic wave where the current is predominantly controlled by charge transfer (Fig. 7). Figures 7(a) and (b) are the results

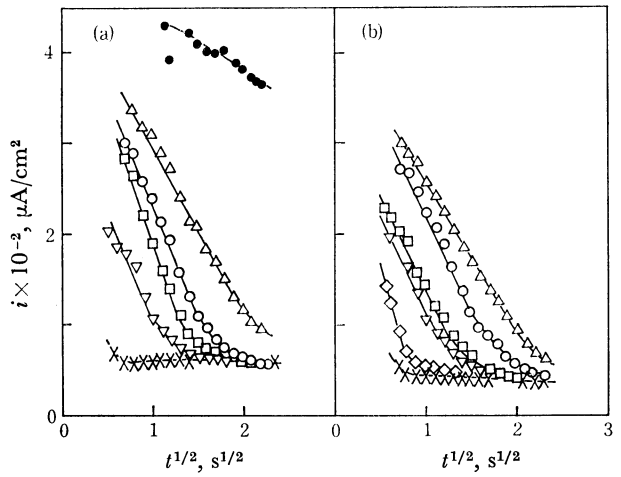


Fig. 7. Instantaneous current density *vs.* square root of time curves for $KBrO_3$ reduction inhibited by polymers. 0.05 M sulfuric acid+1.0 mM $KBrO_3$+polymers, $E=-0.3$ V,
(a) contents of PEG $\bar{M}=8400$ (●: 0 mg/l, △: 25 mg/l, ○: 35 mg/l, □: 40 mg/l, ▽: 50 mg/l, ×: 200 or 300 mg/l),
(b) contents of Triton X-405 $\bar{M}=2000$ (△: 15 mg/l, ○: 20 mg/l, □: 25 mg/l, ▽: 30 mg/l, ◇: 50 mg/l, ×: 70 or 100 mg/l).

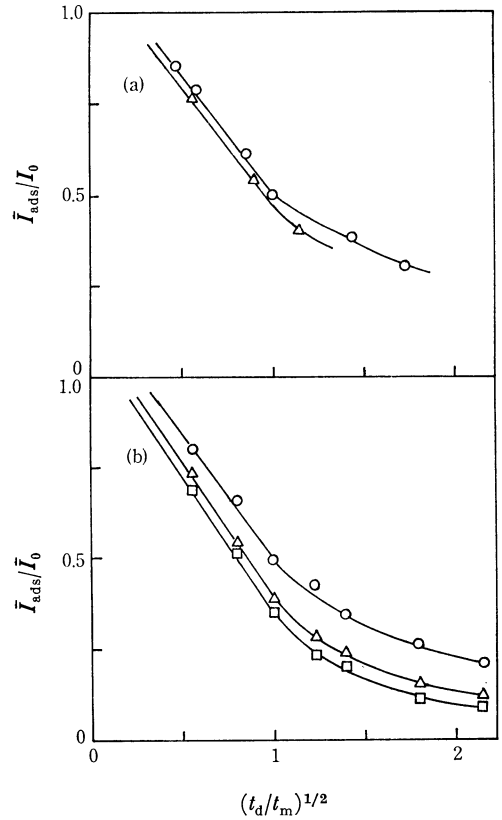


Fig. 8. $(\bar{I}_{ads}/I_0)$ *vs.* $(t_d/t_m)^{1/2}$ plots for $KBrO_3$ reduction in the presence of polymer.
(a) 0.05 M sulfuric acid+1.0 mM $KBrO_3$+PVP (○: $\bar{M}=10000$, △: $\bar{M}=750000$), $E=-0.3$ V,
(b) 0.05 M sulfuric acid+1.0 mM $KBrO_3$+Triton X-205 $\bar{M}=1100$, (○: observed at −0.2 V, △: −0.3 V, □: −0.4 V).

with PEG of $\bar{M}=8400$ and Triton X-405 of $\bar{M}=2000$. In the solution containing adsorbates, $i$ decreases linearly with $t^{1/2}$ in the range of the diffusion-controlled adsorption prior to the saturated adsorption where nearly constant $i$ of *ca.* 60 μA/cm² is obtained, while roughly constant $i$ of *ca.* 400 μA/cm² is observed for the solution without polymer. These phenomena can be explained well by Eqs. (1) and (2).

On the relationships introduced in the foregoing paragraph, $\bar{I}_{ads}/\bar{I}_0$ *vs.* $(t_d/t_m)^{1/2}$ plots are shown in Fig. 8. For $t_d \leqslant t_m$, these plots result in a linear relation having the intercept of *ca.* 1, while for $t_d > t_m$, they approach to the asymptotic value of $i_1/i_0$, as expected from Eq. (3) or (4), respectively. The slopes of Eq. (3) and the asymptotic values of Eq. (4) for $t \to \infty$ obtained from $\bar{I}_{ads}/\bar{I}_0$ *vs.* $(t_d/t_m)^{1/2}$ plots are shown in Table 1, in comparison with those calculated from the instantaneous current densities at −0.3 V. The intercepts of Eq. (3) obtained by $\bar{I}_{ads}/\bar{I}_0$ *vs.* $(t_d/t_m)^{1/2}$ plots are also listed in Table 1. The slopes and the asymptotic values obtained from the figures like Fig. 8 agree approximately with those calculated with the instantaneous current densities except for the slopes with PVP. The intercept values at $t=0$ obtained from $\bar{I}_{ads}/\bar{I}_0$ *vs.* $(t_d/t_m)^{1/2}$ plots are somewhat larger than the theoretical values of unity expected from Eq. (3). Then, it follows that the current density $(i_0)$ on free surface in the solution containing adsorbates is somewhat higher than that $(i_0')$ in the solution without adsorbates, though Eq. (3) holds on the assumption of $i_0=i_0'$ (*cf.* the derivation of Eq. (3)). Such results might be attributed to the interaction between adsorbates and depolarizer on the surface or to the characteristics of capillary.[10]

Table 1. Slopes, asymptotic values, and intercepts of $\bar{I}_{ads}/\bar{I}_0$ *vs.* $(t_d/t_m)^{1/2}$ plots

| Adsorbates | | −E,V | Slopes[a] for $t_d \leq t_m$ | | Asymp. value for $t \to \infty$ | | Intercept at $t=0$ |
|---|---|---|---|---|---|---|---|
| | | | obsd[b] | calcd[c] | obsd[b] | calcd[c] | |
| PEG $\bar{M}=$ | 1000 | 0.3 | 0.74 | 0.60 | 0.22 | 0.22 | 1.02 |
| $\bar{M}=$ | 8400 | 0.3 | 0.74 | 0.67 | 0.18 | 0.13 | 1.08 |
| PVP $\bar{M}=$ | 10000 | 0.3 | 0.73 | 0.41 | 0.27 | 0.27 | 1.20 |
| $\bar{M}=$ | 750000 | 0.3 | 0.74 | 0.46 | 0.25 | 0.33 | 1.20 |
| Triton | X-205 | 0.3 | 0.79 | 0.71 | 0.10 | 0.08 | 1.18 |
| | X-405 | 0.3 | 0.77 | 0.69 | 0.18 | 0.10 | 1.09 |

a) Absolute values. b) The values observed directly from $\bar{I}_{ads}/\bar{I}_0$ *vs.* $(t_d/t_m)^{1/2}$ plots. c) The values calculated from instantaneous current densities (slope=$\frac{10}{13}\frac{i_0-i_1}{i_0}$, asymptotic value=$i_1/i_0$).

Table 2 shows the values of $\alpha n$ and $E''_{1/2}$ (half-wave potential at the saturated adsorption) for the inhibition effects of polymer on $BrO_3^-$ reduction. The values of $\alpha n$ were obtained from the potential dependence of log $(\bar{I}_d-\bar{I}_{ads})/\bar{I}_{ads}$, where $\alpha$, $n$, and $\bar{I}_d$ were the transfer coefficient, the number of electrons involved in the reduction, and the polarographic limiting current. From the results of $E_{1/2}''$ and $\alpha n$ in Table 2, Triton X is found to be most effective on the inhibition of $BrO_3^-$ reduction. The shift of half-wave potential in the presence of

Table 2. Half-wave potential at maximum shift $E''_{1/2}$ and $\alpha n$ for $BrO_3^-$ electroreduction under saturated adsorption of polymers

| Adsorbates | $a$ mg/l | $-E''_{1/2}$, V | $\alpha n^{a)}$ |
|---|---|---|---|
| PEG $\bar{M}$= 1000 | 45 | 0.82 | 0.18 |
| $\bar{M}$= 8400 | 200 | 0.97 | 0.15 |
| PVP $\bar{M}$= 10000 | 300 | 0.67 | 0.19 |
| $\bar{M}$=750000 | 600 | 0.68 | 0.19 |
| Triton X-205 | 250 | 1.20 | 0.14 |
| X-405 | 300 | 0.88 | 0.16 |

In the solution without adsorbates, half-wave potential and $\alpha n$ for $BrO_3^-$ reduction are $-0.40$ V and 0.23.
a) The values of $\alpha n$ are calculated from the relation of $\log\{(\bar{I}_d-\bar{I}_{ads})/\bar{I}_{ads}\}$ *vs.* $E$.

polymer will be derived from the change of the apparent rate constant ($k_{app}$) with polymer and its potential dependence. The instantaneous current in the absence of polymer is given by,

$$I_0 = nFAk_0a^* \tag{5}$$

where $k_0$ and $a^*$ are the rate constant at $\theta=0$ and the concentration at electrode surface.

For the case with polymer,

$$I_{ads} = nFAk_{app}a^* \tag{6}$$

The apparent rate constant can be assumed as the sum of rate constants on covered ($k_1$) and uncovered surface ($k_0$) as follows,[11]

$$k_{app} = k_0(1-\theta) + k_1\theta = k_0 - (k_0-k_1)(t/t_m)^{1/2} \quad \text{for } t \leqslant t_m \tag{7}$$

$$k_{app} = k_1 \quad \text{for } t > t_m \tag{8}$$

Then,

$$(I_{ads})_A = nFAa^*\{k_0-(k_0-k_1)(t/t_m)^{1/2}\} \quad \text{for } t \leqslant t_m \tag{9}$$

or $$I_{(ads)_B} = nFAk_1a^* \quad \text{for } t > t_m \tag{10}$$

The potential dependence of $k_0$ or $k_1$ is expressed as follows,

$$k_0 = k_0^s \exp\left\{-\frac{\alpha nF}{RT}(E-E_0)\right\} \tag{11}$$

$$k_1 = k_1^s \exp\left\{-\frac{\alpha nF}{RT}(E-E_0)\right\} \tag{12}$$

where $k_0^s$ and $k_1^s$ are the standard rate constants for $\theta=0$ and 1, and $E_0$ the standard potential of the system in question. The concentration at the electrode surface can be expressed by the instantaneous current, that is,

$$a^* = \frac{\delta}{D}(I_d-I_0) \tag{13}$$

where $D$ and $\delta$ are the diffusion coefficient and the thickness of diffusion layer.

(a) Potential *vs.* polarographic current relation in the absence of adsorbates; Substituting Eqs. (11) and (13) into the expression for the polarographic current $\bar{I}_0$ which is given by integrating Eq. (5) and dividing its results by the drop life, we can obtain the potential *vs.* polarographic current relation.

$$E = E_0 + \frac{RT}{\alpha nF}\ln(0.85m^{2/3}nF\bar{\delta}D^{-1}) + \frac{RT}{\alpha nF}\ln\frac{\bar{I}_d-\bar{I}_0}{\bar{I}_0} + \frac{RT}{\alpha nF}\ln\frac{3}{5}k_0^s t_d^{2/3} \tag{14}$$

(b) Potential *vs.* polarographic current relation in the presence of adsorbates; When $t_d \leqslant t_m$, the $E-\bar{I}$ relation is given by substituting Eqs. (11), (12), and (13) into the polarographic current of $\bar{I}_{ads}$ obtained from Eq. (9),

$$E = E_0 + \frac{RT}{\alpha nF}\ln(0.85m^{2/3}nF\bar{\delta}D^{-1}) + \frac{RT}{\alpha nF}\ln\frac{\bar{I}_d-\bar{I}_{ads}}{\bar{I}_{ads}} + \frac{RT}{\alpha nF}\ln\left\{\frac{3}{5}k_0^s t_d^{2/3} - \frac{6}{13}(k_0^s-k_1^s)t_m^{-1/2}t_d^{7/6}\right\} \quad \text{for } t_d \leqslant t_m \tag{15}$$

When $t_d > t_m$, the polarographic current of $\bar{I}_{ads}$ is the sum of $(\bar{I}_{ads})_A = \frac{1}{t_d}\int_0^{t_m}(I_{ads})_A\,dt$ and $(\bar{I}_{ads})_B = \frac{1}{t_d}\int_{t_m}^{t_d}(I_{ads})_B\,dt$. Substituting Eqs. (11), (12), and (13) into $\bar{I}_{ads}$ above mentioned, we obtain

$$E = E_0 + \frac{RT}{\alpha nF}\ln(0.85m^{2/3}nF\bar{\delta}D^{-1}) + \frac{RT}{\alpha nF}\ln\frac{\bar{I}_d-\bar{I}_{ads}}{\bar{I}_{ads}} + \frac{RT}{\alpha nF}\ln\left\{\frac{9}{65}(k_0^s-k_1^s)t_m^{5/3}t_d^{-1} + \frac{3}{5}k_1^s t_d^{2/3}\right\} \quad \text{for } t_d > t_m \tag{16}**$$

The half-wave potentials $E_{1/2}$ without polymer and $E'_{1/2}$ with polymer can be derived from Eqs. (14), (15), and (16) by putting $\bar{I}_0=1/2\bar{I}_d$ and $\bar{I}_{ads}=1/2\bar{I}_d$, respectively. Thus, the shift of half-wave potential ($\Delta E_{1/2}=E'_{1/2}-E_{1/2}$) is shown as follows,

$$\Delta E_{1/2} = \frac{RT}{\alpha nF}\ln\left\{1-\frac{10}{13}\left(1-\frac{k_1^s}{k_0^s}\right)\left(\frac{t_d}{t_m}\right)^{1/2}\right\} \quad \text{for } t_d \leqslant t_m \tag{17}$$

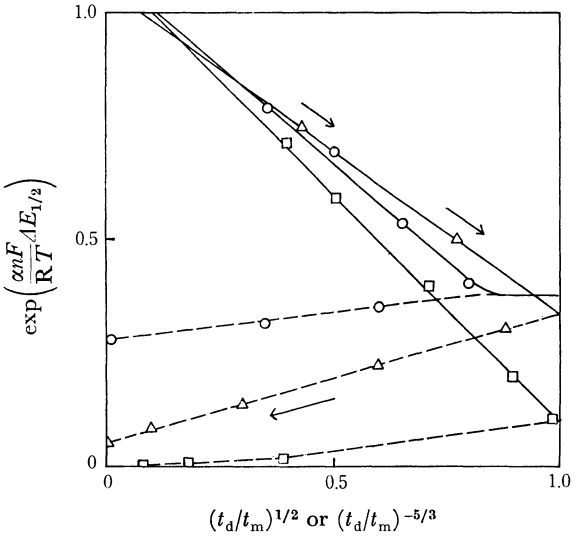


Fig. 9. Shifts of half-wave potential for $KBrO_3$ reduction in the presence of polymers.
0.05 M sulfuric acid+$KBrO_3$+polymers (○: 1.5 mM $KBrO_3$ with various content of PVP $\bar{M}$=10000, △: 1.0 mM $KBrO_3$ with PEG $\bar{M}$=8400, □: 1.0 mM $KBrO_3$ with TritonX-205 $\bar{M}$=1100),
solid lines: $\exp\left(\frac{\alpha nF}{RT}\Delta E_{1/2}\right)$ *vs.* $(t_d/t_m)^{1/2}$ plots, dashed lines: $\exp\left(\frac{\alpha nF}{RT}\Delta E_{1/2}\right)$ *vs.* $(t_d/t_m)^{-5/3}$ plots.

** $t_d\bar{I}_{ads} = \int_0^{t_m}(I_{ads})_A dt + \int_{t_m}^{t_d}(I_{ads})_B dt$

or

$$\Delta E_{1/2} = \frac{RT}{\alpha nF} \ln\left[\frac{k_1^s}{k_0^s} + \left\{1 - \frac{k_1^s}{k_0^s} - \frac{10}{13}\left(1 - \frac{k_1^s}{k_0^s}\right)\right\}\left(\frac{t_d}{t_m}\right)^{-5/3}\right] \quad \text{for } t_d > t_m \qquad (18)$$

On the basis of these relationships, the plots of $\exp\left(\frac{\alpha nF}{RT}\Delta E_{1/2}\right)$ *vs.* $(t_d/t_m)^{1/2}$ or $(t_d/t_m)^{-5/3}$ are shown in Fig. 9, where the arrows indicate the increase of adsorbates contents.

Since $\exp\left(\frac{\alpha nF}{RT}\Delta E_{1/2}\right)$ decreases linearly with $(t_d/t_m)^{1/2}$ for $t_d \leqslant t_m$ and increases with $(t_d/t_m)^{-5/3}$ for $t_d > t_m$, the shift of $E_{1/2}$ is explained by Eq. (17) or (18).

*Examination of Eq. (17) or (18) for the Inhibition Effects of Polymers on Cation Reduction.* The characteristics for the inhibition effects of polymer on the electroreduction are assumed to be independent of the ionic charge of depolarizer except for the double layer effects within the potential range where the current is predominantly controlled by charge transfer. In the irreversible reduction of $VO^{2+}$, the polarogram in the acetate

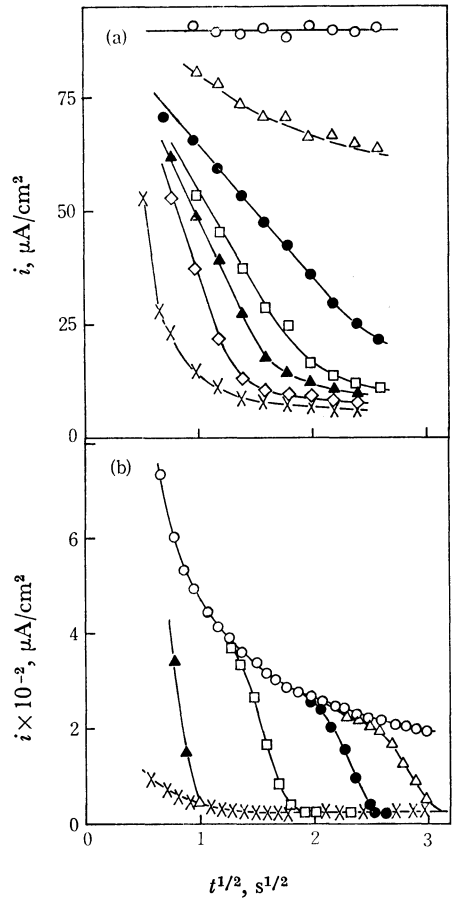


Fig. 10. Instantaneous current density *vs.* square root of time curves for cation reduction inhibited by polymer.
(a) (0.5 M $CH_3COOH$+0.5 M $CH_3COONa$)+1.0 mM $VOSO_4$+PVP $\bar{M}$=750000, $E=-1.1$ V, contents of PVP (○: 0 mg/l, △: 80 mg/l, ●: 110 mg/l, □: 140 mg/l, ▲: 170 mg/l, ◇: 250 mg/l, ×: 500 mg/l),
(b) 1 N sulfuric acid+1.0 mM $CdSO_4$+PVP $\bar{M}$=750000, $E=-0.9$ V, contents of PVP (○: 0 mg/l, △: 80 mg/l, ●: 100 mg/l, □: 150 mg/l, ▲: 400 mg/l, ×: 800 mg/l).

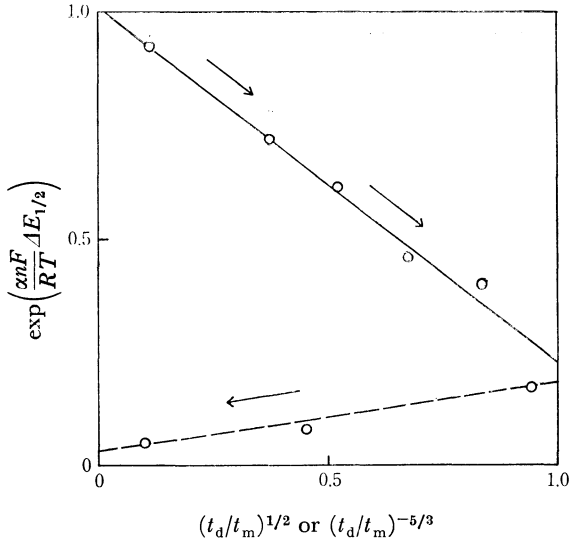


Fig. 11. Shift of half-wave potential for $VOSO_4$ reduction in the presence of polymers.
(0.5 M $CH_3COOH$+0.5 M $CH_3COONa$)+1.0 mM $VOSO_4$+various contents of PVP $\bar{M}$=750000, Solid line: $\exp\left(\frac{\alpha nF}{RT}\Delta E_{1/2}\right)$ *vs.* $(t_d/t_m)^{1/2}$ plot, dashed line: $\exp\left(\frac{\alpha nF}{RT}\Delta E_{1/2}\right)$ *vs.* $(t_d/t_m)^{-5/3}$ plots.

buffer of pH 4.7 was inhibited by the polymer in the same way as that for $BrO_3^-$, that is, the half-wave potential became more negative with the addition of the polymers. In this case, the exact determination of $t_m$ was possible by the $i-t^{1/2}$ plot shown in Fig. 10(a) in the potential range where the charge transfer was predominant. The results in Fig. 10(a) show that Eqs.(1) and (2) hold well for the inhibited reduction of $VO^{2+}$ where the current is mainly controlled by charge transfer. Then, it follows that Eq. (17) or (18) based on Eq. (1) or (2) is applicable to the above case. In Fig. 11, the plot of $\exp\left(\frac{\alpha nF}{RT}\Delta E_{1/2}\right)$ *vs.* $(t_d/t_m)^{1/2}$ or $(t_d/t_m)^{-5/3}$ becomes linear as expected from Eq. (17) or (18), respectively. The arrows in the figure indicate the increase of adsorbate contents. Meantime, typical results in contrast with $i-t^{1/2}$ plots in Fig. 10(a) are shown in Fig. 10(b), which reveals the inhibition effects of polymer on the instantaneous limiting current density of $Cd^{2+}$ reduction. In the absence of adsorbates, the results reveal the process mainly controlled by linear diffusion of depolarizer, since the instantaneous current density decreases with the function of $1/t^{1/2}$ which is expected from the Ilković equation.[12] In the presence of adsorbates, the depression of instantaneous current density is not expressed as a linear relation of $i$ *vs.* $t^{1/2}$ which implies the blocking effect of polymer, but shows the sharp change after a certain adsorption time. Such results may be due to the inhibition which is dependent not only on the blocking effect of adsorbates but also on the variation of diffusion path of depolarizer having fast reaction rate.[3]

*Summary.* So far as the present research is concerned, the inhibition effects of polymer on reduction current may be classified into two typical cases regard-

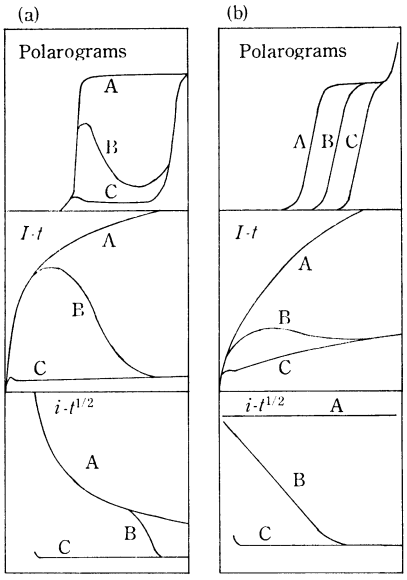


Fig. 12. Models for inhibition effects of polymer on electroreduction current.
A: with no polymer, B: with polymer in the case of diffusion-controlled adsorption, C: with polymer in the case of saturated adsorption,
(a) inhibition effects on reaction in the potential ranges of limiting current,
(b) inhibition effects on reaction in the potential ranges where the current is mainly controlled by charge transfer.

less of the ionic charge of depolarizer. Fig. 12(a) shows the typical inhibition effects of polymer when the current is predominantly controlled by mass transfer of ions. In such a case, the time $t_m$ needed to complete a monolayer of polymer can be obtained directly from $I-t$ curve, which results in a convenient determination of $\Gamma_m$ of polymer. In these cases, $i-t^{1/2}$ plots differ markedly from those in Fig. 12(b) for the process mainly controlled by charge transfer. Meanwhile, Fig. 12(b) shows the other type of inhibition effects of polymer when the current is mainly controlled by charge transfer. In such cases, the time $t_m$ can be obtained exactly from $i-t^{1/2}$ relation instead of $I-t$ curve.

Moreover, Eqs. (17) and (18) for the shift of half-wave potential in the presence of adsorbates were verified with regard to the system of Fig. 12(b), *i.e.*, the inhibition effects of polymer on the electroreduction of $BrO_3^-$ or $VO^{2+}$.

## References

1) T. Yoshida, T. Ohsaka, and S. Tanaka, This Bulletin, **45**, 362 (1972); T. Yoshida, T. Ohsaka, and S. Nomoto, *ibid.*, **45**, 1585 (1972).
2) T. Yoshida, T. Ohsaka, and M. Suzuki, *ibid.*, **45**, 3245 (1972).
3) T. Ohsaka, H. Yamamoto, and T. Yoshida, *ibid.*, **46**, 1320 (1973).
4) A. N. Frumkin and G. M. Florianovich, *Zh. Fiz. Khim.*, **29**, 1827 (1955).
5) T. N. Anderson and H. Eyring, "Physical Chemistry an Advanced Treatise," Vol. IXA, ed. by H. Eyring, D. Henderson, and W. Jost, Academic Press, New York, (1960), p. 310; R. Parsons, "Advances in Electrochemistry and Electrochemical Engineering," Vol. 1, ed. by P. Delahay and C. W. Tobias, Interscience Publishers, New York, (1961), p. 41.
6) A. N. Frumkin, *Z. Electrochem.*, **59**, 807 (1955); I. Müller, *Electrochim. Acta.*, **14**, 293 (1969).
7) J. J. Lingane and I. M. Kolthoff, *J. Amer. Chem. Soc.*, **61** 825 (1939); V. I. Zykov, *Dokl. Akad. Nauk SSSR*, **136**, 1158 (1961); A. M. Shams El Din, T. M. H. Saber, and H. A. El Shayeb, *J. Electroanal. Chem.*, **36**, 411 (1972).
8) T. Yoshida and T. Ohsaka, *Bull. Sci. Eng. Res. Lab. Waseda Univ.*, **58**, 34 (1972).
9) J. Koryta, *Collect. Czech. Chem. Commun.*, **18**, 206 (1953).
10) J. Kůta and I. Smoler, "Progress in Polarography," Vol. 1, ed. by P. Zuman and I. M. Kolthoff, Interscience Publishers, New York, (1962), p. 49.
11) J. Kůta, J. Weber, and J. Koutecký, *Collect. Czech. Chem. Commun.*, **25**, 2376 (1960); J. Kůta and I. Smoler, *Z. Electrochem.*, **64**, 285 (1960).
12) L. Meites, "Polarographic Techniques," Second Ed., Interscience Publishers, New York, (1965), p. 113.